

# Slot waveguides with polycrystalline silicon for electrical injection

Kyle Preston and Michal Lipson\*

School of Electrical and Computer Engineering, Cornell University, Ithaca, N.Y. 14853

Corresponding author: [lipson@ece.cornell.edu](mailto:lipson@ece.cornell.edu)

**Abstract:** We demonstrate horizontal slot waveguides using high-index layers of polycrystalline and single crystalline silicon separated by a 10 nm layer of silicon dioxide. We measure waveguide propagation loss of 7 dB/cm and a ring resonator intrinsic quality factor of 83,000. The electric field of the optical mode is strongly enhanced in the low-index oxide layer, which can be used to induce a strong modal gain when an active material is embedded in the slot. Both high-index layers are made of electrically conductive silicon which can efficiently transport charge to the slot region. The incorporation of conductive silicon materials with high- $Q$  slot waveguide cavities is a key step for realizing electrical tunneling devices such as electrically pumped silicon-based light sources.

©2009 Optical Society of America

**OCIS codes:** (130.3130) Integrated optics materials; (230.5750) Resonators; (130.3120) Integrated optical devices.

---

## References and links

1. L. Pavesi, "Silicon-Based Light Sources for Silicon Integrated Circuits," *Advances in Optical Technologies* (2008).
2. A. W. Fang, H. Park, O. Cohen, R. Jones, M. J. Paniccia, and J. E. Bowers, "Electrically pumped hybrid AlGaInAs-silicon evanescent laser," *Opt. Express* **14**, 9203-9210 (2006).
3. P. Rojo Romeo, J. Van Campenhout, P. Regreny, A. Kazmierczak, C. Seassal, X. Letartre, G. Hollinger, D. Van Thourhout, R. Baets, J. M. Fedeli, and L. Di Cioccio, "Heterogeneous integration of electrically driven microdisk based laser sources for optical interconnects and photonic ICs," *Opt. Express* **14**, 3864-3871 (2006).
4. T. Kitagawa, K. Hattori, M. Shimizu, Y. Ohmori, and M. Kobayashi, "Guided-wave laser based on erbium-doped silica planar lightwave circuit," *Electron. Lett.* **27**, 334-335 (1991).
5. A. Polman, B. Min, J. Kalkman, T. J. Kippenberg, and K. J. Vahala, "Ultralow-threshold erbium-implanted toroidal microlaser on silicon," *Appl. Phys. Lett.* **84**, 1037-1039 (2004).
6. C. A. Barrios and M. Lipson, "Electrically driven silicon resonant light emitting device based on slot-waveguide," *Opt. Express* **13**, 10092-10101 (2005).
7. M. Galli, A. Politi, M. Belotti, D. Gerace, M. Liscidini, M. Patrini, L. C. Andreani, M. Miritello, A. Irrera, F. Priolo, and Y. Chen, "Strong enhancement of  $\text{Er}^{3+}$  emission at room temperature in silicon-on-insulator photonic crystal waveguides," *Appl. Phys. Lett.* **88**, 251114 (2006).
8. M. Galli, D. Gerace, A. Politi, M. Liscidini, M. Patrini, L. C. Andreani, A. Canino, M. Miritello, R. L. Savio, A. Irrera, and F. Priolo, "Direct evidence of light confinement and emission enhancement in active silicon-on-insulator slot waveguides," *Appl. Phys. Lett.* **89**, 241114 (2006).
9. V. R. Almeida, Q. Xu, C. A. Barrios, and M. Lipson, "Guiding and confining light in void nanostructure," *Opt. Lett.* **29**, 1209-1211 (2004).
10. Q. Xu, V. R. Almeida, R. R. Panepucci, and M. Lipson, "Experimental demonstration of guiding and confining light in nanometer-size low-refractive-index material," *Opt. Lett.* **29**, 1626-1628 (2004).
11. J. T. Robinson, K. Preston, O. Painter, and M. Lipson, "First-principle derivation of gain in high-index-contrast waveguides," *Opt. Express* **16**, 16659-16669 (2008).
12. M. Fujii, M. Yoshida, Y. Kanzawa, S. Hayashi, and K. Yamamoto, "1.54  $\mu\text{m}$  photoluminescence of  $\text{Er}^{3+}$  doped into  $\text{SiO}_2$  films containing Si nanocrystals: Evidence for energy transfer from Si nanocrystals to  $\text{Er}^{3+}$ ," *Appl. Phys. Lett.* **71**, 1198-1200 (1997).
13. L. D. Negro, R. Li, J. Warga, and S. N. Basu, "Sensitized erbium emission from silicon-rich nitride/silicon superlattice structures," *Appl. Phys. Lett.* **92**, 181105 (2008).
14. R. Sun, P. Dong, N. N. Feng, C. Y. Hong, J. Michel, M. Lipson, and L. Kimerling, "Horizontal single and multiple slot waveguides: optical transmission at  $\lambda = 1550$  nm," *Opt. Express* **15**, 17967-17972 (2007).

15. E. Jordana, J. M. Fedeli, P. Lyan, J. P. Colonna, P. E. Gautier, N. Daldosso, L. Pavesi, Y. Lebour, P. Pellegrino, B. Garrido, J. Blasco, F. Cuesta-Soto, and P. Sanchis, "Deep-UV Lithography Fabrication of Slot Waveguides and Sandwiched Waveguides for Nonlinear Applications," in *Group IV Photonics* (IEEE, 2007), pp.222-224.
16. R. M. Pafchek, J. Li, R. S. Tummidi, and T. L. Koch, "Low loss Si-SiO<sub>2</sub>-Si 8nm slot waveguides," in Conference on Lasers and Electro-Optics (Optical Society of America, 2008), paper CThT3.
17. Y. Lebour, R. Guider, E. Jordana, J.-M. Fedeli, P. Pellegrino, S. Hernandez, B. Garrido, N. Daldosso, and L. Pavesi, "High quality coupled ring resonators based on silicon clusters slot waveguide," in *Group IV Photonics* (IEEE, 2008), pp.215-217.
18. J. B. Lasky, "Wafer bonding for silicon-on-insulator technologies," *Appl. Phys. Lett.* **48**, 78-80 (1986).
19. P. Sangwoo, S. Taichi, J. P. Denton, and G. W. Neudeck, "Multiple layers of silicon-on-insulator islands fabrication by selective epitaxial growth," *IEEE Electron Device Lett.* **20**, 194-196 (1999).
20. P. Koonath, T. Indukuri, and B. Jalali, "Monolithic 3-D Silicon Photonics," *J. Lightwave Technol.* **24**, 1796 (2006).
21. G. Cocorullo, F. G. Della Corte, R. de Rosa, I. Rendina, A. Rubino, and E. Terzini, "Amorphous silicon-based guided-wave passive and active devices for silicon integrated optoelectronics," *IEEE J. Sel. Top. Quantum Electron.* **4**, 997-1002 (1998).
22. R. Orobtcouk, S. Jeannot, B. Han, T. Benyattou, J. M. Fedeli, and P. Mur, "Ultra compact optical link made in amorphous silicon waveguide," *Proc. SPIE* **6183**, 618304-618310 (2006).
23. D. K. Sparacin, R. Sun, A. M. Agarwal, M. A. Beals, J. Michel, L. C. Kimerling, T. J. Conway, A. T. Pomerene, D. N. Carothers, M. J. Grove, D. M. Gill, M. S. Rasras, S. S. Patel, and A. E. White, "Low-Loss Amorphous Silicon Channel Waveguides for Integrated Photonics," in *Group IV Photonics* (IEEE, 2006), pp.255-257.
24. R. A. Street, *Hydrogenated Amorphous Silicon* (Cambridge University Press, 1991).
25. T. Kamins, *Polycrystalline Silicon for Integrated Circuits and Displays*, 2nd ed. (Kluwer, 1998).
26. L. Liao, D. R. Lim, A. M. Agarwal, X. Duan, K. K. Lee, and L. C. Kimerling, "Optical transmission losses in polycrystalline silicon strip waveguides," *J. Electron. Mater.* **29**, 1380-1386 (2000).
27. K. Preston, B. Schmidt, and M. Lipson, "Polysilicon photonic resonators for large-scale 3D integration of optical networks," *Opt. Express* **15**, 17283-17290 (2007).
28. Q. Fang, J. F. Song, S. H. Tao, M. B. Yu, G. Q. Lo, and D. L. Kwong, "Low loss (~6.45dB/cm) sub-micron polycrystalline silicon waveguide integrated with efficient SiON waveguide coupler," *Opt. Express* **16**, 6425-6432 (2008).
29. V. R. Almeida, R. R. Panepucci, and M. Lipson, "Nanotaper for compact mode conversion," *Opt. Lett.* **28**, 1302-1304 (2003).
30. A. Nitkowski, L. Chen, and M. Lipson, "Cavity-enhanced on-chip absorption spectroscopy using microring resonators," *Opt. Express* **16**, 11930-11936 (2008).
31. F. Dell'Olio and V. M. Passaro, "Optical sensing by optimized silicon slot waveguides," *Opt. Express* **15**, 4977-4993 (2007).
32. W. J. Miniscalco, "Erbium-doped glasses for fiber amplifiers at 1500 nm," *J. Lightwave Technol.* **9**, 234-250 (1991).
33. E. Snoeks, G. N. van den Hoven, and A. Polman, "Optimization of an Er-doped silica glass optical waveguide amplifier," *IEEE J. Quantum Electron.* **32**, 1680-1684 (1996).
34. M. Borselli, T. Johnson, and O. Painter, "Beyond the Rayleigh scattering limit in high-Q silicon microdisks: theory and experiment," *Opt. Express* **13**, 1515-1530 (2005).
35. D. K. Sparacin, S. J. Spector, and L. C. Kimerling, "Silicon waveguide sidewall smoothing by wet chemical oxidation," *J. Lightwave Technol.* **23**, 2455-2461 (2005).

## 1. Introduction

The remaining critical capabilities yet to be demonstrated on the integrated silicon photonic platform using standard microelectronic fabrication processes are electrically pumped amplification and lasing within a silicon waveguide [1]. Silicon is an excellent waveguide material because it is transparent in the telecommunications band at  $\lambda = 1550$  nm and can be processed inexpensively, but it is a poor gain material due to its indirect bandgap. Therefore it is advantageous to combine a silicon waveguide structure with a more efficient 1550 nm gain material for on-chip applications. Electrically pumped lasers have been demonstrated with III-V materials evanescently coupled to a silicon waveguide [2, 3], however these approaches rely on a wafer bonding step which is low throughput and not currently a standard microelectronic fabrication process. Optically pumped lasing has been shown in erbium-

doped oxide structures [4, 5], but electrical pumping of insulating materials is not straightforward.

One possible solution for electrically pumped amplification within a silicon waveguide is to combine an erbium-doped insulator with the slot waveguide geometry [6-8]. A slot waveguide is formed by separating two regions of high refractive index by a subwavelength slot of low refractive index. A guided optical mode with a polarization normal to the slot interface (the “slot mode”) has a large electric field enhancement within the low-index slot region [9, 10] which supports an efficient conversion of material gain to modal gain [11]. Figure 1 demonstrates the field enhancement in a horizontal slot of silicon dioxide ( $n = 1.46$ ) in a silicon waveguide ( $n = 3.48$ ). The low-index region could be an erbium-doped silicon-rich oxide [12] or nitride [13] that is electrically excited by carrier tunneling through the slot region and emits into the waveguide mode. Erbium-doped films can be fabricated by standard techniques such as ion implantation or sputter deposition and do not require a wafer bonding step. Previous work in amorphous silicon slot waveguides has yielded promising optical results [14-17], however the typical electrical mobility is too low for an efficient on-chip electrical device. In this paper we design, analyze, and experimentally demonstrate a novel silicon slot waveguide structure with geometry and materials suitable for electrical pumping of an active gain material.

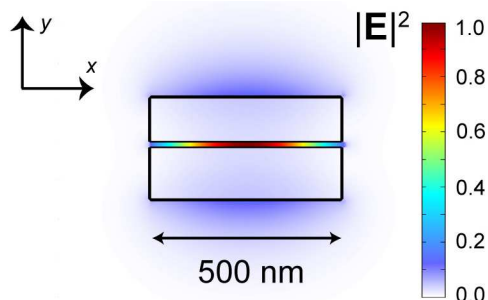


Fig. 1.  $|E|^2$  of the fundamental  $y$ -polarized quasi-TM slot mode at  $\lambda = 1550$  nm as calculated by a finite difference mode solver. The high-index regions (bounded by black) have  $n_{Si} = 3.48$  and the slot and cladding have  $n_{oxide} = 1.46$ . The bottom and top silicon layers are 140 nm tall and 120 nm tall respectively, and the slot is 10 nm tall. The effective index is  $n_{eff} = 1.87$  and the slot confinement factor is  $\Gamma = 0.28$ .

## 2. Design and fabrication

The key considerations in designing a slot waveguide suitable for electrical injection are the waveguide geometry, orientation, and choice of materials. To keep the operating voltage of the proposed device at reasonable levels, we choose the size of the oxide slot to be 10 nm. This allows for future electrical excitation of a gain material by Fowler-Nordheim tunneling through oxide with a voltage drop across the slot on the order of volts, since the onset of tunneling is typically around  $5 \text{ MV/cm} = 0.5 \text{ V/nm}$  of tunneling distance [6]. In order to achieve low losses with such a small slot size, we choose the horizontal slot configuration. This way the different waveguide regions can be formed by deposition or growth techniques with nanometer-scale accuracy and sub-nanometer surface roughness. This is in contrast to a vertical slot which must be defined lithographically and etched down into a silicon waveguide [9, 10] which is difficult for a slot size below 50 nm.

We choose a top layer of polycrystalline silicon (polysilicon) to provide good electrical conductivity for the device. Ideally, crystalline silicon (c-Si) would be used for both the top and bottom layers, but multiple layers of c-Si can only be obtained by nonstandard techniques such as wafer bonding [18], epitaxial overgrowth [19], or oxygen implantation [20]. Hydrogenated amorphous silicon (a-Si:H) can be used in horizontal slot waveguides with good loss values  $\sim 2\text{-}4 \text{ dB/cm}$  [14-17], but this material is poorly suited for the proposed electrical-injection device due to very low electrical carrier mobility. Optical-quality thin

films of a-Si:H are deposited by plasma enhanced chemical vapor deposition (PECVD) at low temperatures, typically around 200°C [21-23]. At these temperatures a significant atomic percentage of hydrogen is incorporated in the material to fill dangling Si bonds [24] and prevent optical loss by absorption. Despite their excellent optical properties, a-Si:H films suffer from low electrical carrier mobility  $\mu$  on the order of 1 cm<sup>2</sup>/V·s [24] (corresponding to high resistivity  $\rho \sim 1/\mu$ ). In contrast, the electrical mobility of polycrystalline silicon can be much better, on the order of 100 cm<sup>2</sup>/V·s [25]. Drift current density through a material is defined as  $\mathbf{J} = nq\mu\mathbf{E}$  (with  $n$  the carrier density,  $q$  the electron charge, and  $\mathbf{E}$  the voltage per length applied across the material), so a 100x decrease in  $\mu$  implies that a 100x higher voltage will be required to inject the same current  $\mathbf{J}$  through a material. For example, if a voltage drop of a few volts is required across a polysilicon slab connecting a metal contact to the waveguide, then a few hundred volts may be required across a similar a-Si:H electrode. This presents serious design challenges for the realization of a reliable and efficient on-chip device using a-Si:H.

In this work we use a layer of deposited polysilicon, which exhibits good electrical properties. Polysilicon is a standard deposited microelectronic material that consists of crystalline grains separated by disordered grain boundaries. Polysilicon has typically been considered a poor optical material not suitable for low-loss applications because it is inhomogeneous and inherently has some optical loss due to scattering. However, channel waveguides have recently been demonstrated with losses on the order of 10 dB/cm or less [26-28] when the material is processed to have smooth interfaces and a maximized grain size such that only a few grain boundaries are present per waveguide cross-section. Here we demonstrate the first use of optical-quality polysilicon in a slot waveguide configuration, with the primary goal of minimizing the waveguide loss inside a resonator for light emission applications.

Fabrication of the slot waveguides is done on a commercial four-inch silicon-on-insulator wafer. We start with a 250 nm layer of single-crystalline silicon on a 3  $\mu\text{m}$  buried oxide layer, then thin the top silicon layer to 145 nm by thermal oxidation and remove the grown oxide with hydrofluoric acid. Then we grow a 10 nm silicon dioxide layer for the slot region using dry thermal oxidation at 950°C. This leaves a 140 nm bottom layer of c-Si. Using atomic force microscopy (AFM), we measure the root mean squared (rms) roughness of the top oxide interface to be below 0.2 nm. We deposit a 120 nm top layer of amorphous silicon by low pressure chemical vapor deposition (LPCVD) at 550°C and anneal the wafer in N<sub>2</sub> at a maximum temperature of 1100°C to crystallize the film into polysilicon [27]. We determine the rms roughness of the top surface to be 0.5 nm by AFM, as shown in Fig. 2. A cross-sectional transmission electron microscope (TEM) image is shown in Fig. 3, where the polycrystalline nature of the top layer is visible. The layer thicknesses are chosen to optimize the modal confinement  $\Gamma$  in the slot region for the final waveguide structure [11]. To pattern waveguides and resonators, we use e-beam lithography and a 100 nm layer of XR-1541 e-beam resist before etching the structures with chlorine-based inductively coupled plasma reactive ion etching. Finally, we clad the structures in a 3  $\mu\text{m}$  PECVD silicon dioxide layer before dicing and polishing the end facets of the chip.

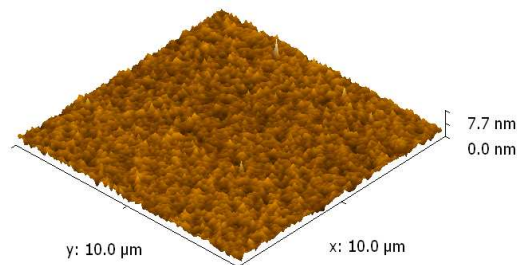


Fig. 2. AFM measurement of the polysilicon top surface over a 10  $\mu\text{m}$  square field. The rms roughness is 0.5 nm and the total range is  $\pm 3.7$  nm from the mean value.

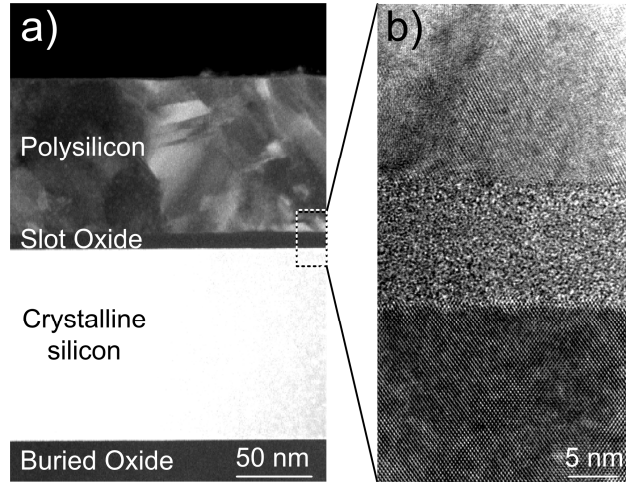


Fig. 3. (a) Dark field STEM (scanning tunneling electron microscope) image of the fabricated material stack. (b) Bright field TEM image of the slot region showing the polycrystalline, amorphous, and single crystalline layers (top to bottom).

### 3. Experimental results

We measure the loss in 500 nm-wide waveguides (see Fig. 1) by employing the cutback method with multiple waveguides of increasing path length. Light from a tunable infrared laser passes through a polarization controller and is coupled on- and off-chip using a tapered lens fiber and patterned waveguide nanotapers [29]. Output from the chip is collected by a lens and focused through a polarization filter onto a detector. At a given wavelength, we record the transmission through each waveguide and plot the relative transmission on a logarithmic plot as shown in the inset of Fig. 4. The slope of a linear fit gives the waveguide loss, which we calculate to be 7.3 dB/cm at  $\lambda = 1550$  nm with a standard error of 0.4 dB/cm. Figure 4 shows the same measurement repeated at many wavelengths, and we find losses of around 6-8 dB/cm within the C-band emission window of erbium.

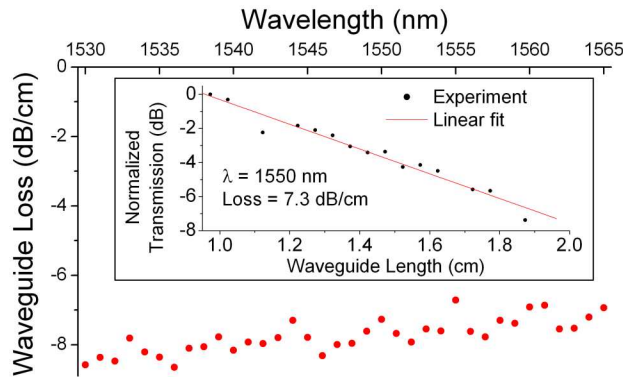


Fig. 4. Measurement of propagation loss in slot waveguides using the cutback method. (inset) Single measurement at  $\lambda = 1550$  nm with a loss of  $7.3 \pm 0.4$  dB/cm.

We also demonstrate high-quality-factor ring resonator cavities based on these horizontal slot waveguides. In order to minimize excess bending, scattering, and coupling loss in the resonator, we choose a 100  $\mu\text{m}$  radius ring coupled to a bus waveguide with a coupling gap of 550 nm as shown in Fig. 5(a). Using the radius of the ring and the measured free spectral range (FSR) as a function of wavelength in the inset of Fig. 5(c), we can calculate the group

index  $n_g(\lambda) = \lambda^2/(FSR \cdot 2\pi R)$  [27]. A comparison to finite difference modal simulations in Fig. 5(b) provides strong experimental evidence that we are indeed operating in the TM-polarized slot mode. A close scan of a resonance at  $\lambda_0 = 1552.12$  nm is shown in Fig. 5(c). We measure a resonant linewidth  $\Delta\lambda_{FWHM} = 29$  pm which corresponds to an undercoupled quality factor  $Q_{loaded} = 54,000$ . We fit this resonance to a Lorentzian of the form [30]:

$$T = \frac{(a-r)^2 + \frac{4\pi^2 raL^2 n_g^2}{\lambda_0^4} (\lambda - \lambda_0)^2}{(1-ra)^2 + \frac{4\pi^2 raL^2 n_g^2}{\lambda_0^4} (\lambda - \lambda_0)^2}. \quad (1)$$

Here  $L$  is the path length around the ring,  $n_g = 3.50$  is the measured group index, and our two fitting parameters are a coupling term  $r$  and a loss term  $a$ . The least squares Lorentzian fit with values  $a = 0.948$  and  $r = 0.978$  is shown in Fig. 4(c). This corresponds to a propagation loss within the ring  $\alpha_{ring} = -2 \ln(a)/L = 1.7 \text{ cm}^{-1} = 7.4 \text{ dB/cm}$  and an intrinsic quality factor  $Q_0 = (2\pi n_g)/(\lambda_0 \alpha_{ring}) = 83,000$  [27]. The loss calculated in the resonator matches closely with the straight waveguide loss measurement in Fig. 3. This indicates that excess bending loss and coupling loss in the resonator are negligible (within the error of the waveguide measurement) due to the large ring radius (100  $\mu\text{m}$ ) and coupling gap (550 nm).

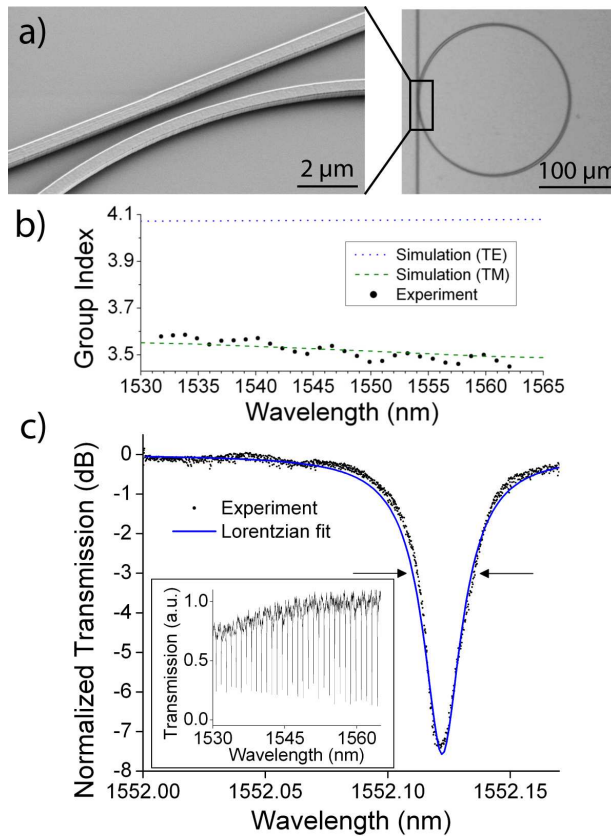


Fig. 5. (a) Tilted angle SEM (before oxide cladding) and optical microscope image of 100  $\mu\text{m}$  radius ring resonator and bus waveguide. (b) Experimental measurement (dots) of the group index based on the measured free spectral range as a function of wavelength. The comparison with simulation indicates we are operating in the TM-polarized slot mode shown in Fig. 1. (c) Resonance at  $\lambda_0 = 1552.12$  nm with intrinsic quality factor  $Q_0 = 82,000$ . (inset) Wider sweep showing  $FSR$  used to calculate group index in (b).

#### 4. Discussion

Slot waveguides are attractive for light emission and amplification because they provide a strong electric field enhancement in the slot region [9, 10] which can be filled with an active material. The mode overlap induces an efficient conversion of the slot's local material gain  $g_{slot}$  to a modal gain  $g_{modal}$ , resulting in a large waveguide power amplification  $P(z) = P(0) \cdot \exp(g_{modal} z)$ . The percent of material gain converted to modal gain is characterized by  $\Gamma = g_{modal} / g_{slot}$ , the confinement factor [11, 31]:

$$\Gamma = \frac{n_{slot} \iint_{slot} |\mathbf{E}|^2 dx dy}{Z_0 \iint_{-\infty}^{\infty} \text{Re}\{\mathbf{E} \times \mathbf{H}\} \cdot \hat{\mathbf{z}} dx dy}. \quad (2)$$

Here  $n_{slot}$  is the real part of the refractive index of the slot region,  $Z_0$  is the impedance of free space,  $\hat{\mathbf{z}}$  is the direction of propagation, and  $\mathbf{E}$  and  $\mathbf{H}$  are the mode's electric and magnetic fields. A slot mode provides high electric field intensity in the slot per unit power in the waveguide, satisfying the condition for large  $\Gamma$  even for a deeply subwavelength slot size that allows for electrical tunneling. We calculate the waveguide presented here to have confinement  $\Gamma = 28\%$  inside the 10 nm slot at  $\lambda = 1550$  nm. This is close to the fully optimized value of  $\Gamma_{max} = 33\%$  for a 10 nm oxide slot in silicon [11].

Based on typical material gain values and our waveguide geometry, we can calculate the minimum waveguide loss  $\alpha$  required to achieve lasing in these structures. Given a typical emission cross section  $\sigma_{Er} = 6 \cdot 10^{-21} \text{ cm}^2$  for erbium ions in silica [32, 33] and an average erbium doping concentration  $n_{Er} = 2 \cdot 10^{20} \text{ cm}^{-3}$  [32, 33], one could expect a material gain  $g_{slot} = \sigma_{Er} \cdot n_{Er} = 1.2 \text{ cm}^{-1} = 5.2 \text{ dB/cm}$  which can be inserted into the slot. Given confinement  $\Gamma = 0.3$  determined by the waveguide geometry, we then require a maximum propagation loss  $\alpha = g_{modal} = \Gamma \cdot g_{slot} = 1.6 \text{ dB/cm}$  in order to reach the laser oscillation condition, or equivalently a minimum resonator intrinsic quality factor  $Q_0 = (2\pi n_g) / (\lambda_0 \alpha) = 400,000$  with  $n_g = 3.5$  and  $\lambda_0 = 1550$  nm.

Future generations of these devices will therefore require either an increase in confinement  $\Gamma$  or a decrease in propagation loss  $\alpha$  to achieve lasing. Waveguides can be designed with multiple slots to increase both  $\Gamma$  and the achievable gain  $g_{modal}$  without significantly increasing the propagation loss  $\alpha$  [14]. The inclusion of two 10 nm slots separated by 50 nm of silicon can result in confinement factors  $\Gamma > 50\%$ , thereby increasing the acceptable waveguide losses to around 3 dB/cm. Several approaches then exist for the moderate loss reduction required from 7 dB/cm to 3 dB/cm. We estimate that 2-3 dB/cm of the current 7 dB/cm loss comes from sidewall scattering and absorption (similar to that seen in c-Si [34]) and the remaining 4-5 dB/cm of waveguide loss is due to material loss (absorption and scattering) in the polysilicon [26]. Several methods used to successfully reduce sidewall loss in c-Si include roughness reduction by e-beam resist smoothing (pre-etching) [34] and waveguide surface smoothing and passivation by oxidation (post-etching) [35]. Additionally, it has been reported that hydrogen passivation of grain boundary states inside polysilicon improves the material loss by several dB/cm [26]. Conservatively, we expect that greater than 50% improvement is achievable in both of the loss categories, which would result in the required overall loss reduction from our measured value of 7 dB/cm.

#### 5. Conclusion

In conclusion, we have demonstrated horizontal slot waveguides and resonators designed for efficient electrical injection by incorporating electrically active high-index materials suitable for electrodes and a 10 nm thin oxide slot suitable for carrier tunneling. This class of structures may enable on-chip silicon-based amplifiers and light sources when combined with a suitable gain material in the slot (such as an erbium-doped silicon-rich oxide or nitride) and a forward-biased PIN diode for carrier injection.

## **Acknowledgments**

The authors gratefully acknowledge C. Manolatu for the use of her finite difference code, J. Grazul for TEM imaging, and J. T. Robinson for productive discussions. This work was sponsored under the U.S. Air Force MURI program on "Electrically Pumped Silicon-Based Lasers for Chip-Scale Nanophotonic Systems" supervised by Dr. Gernot Pomrenke. This work was performed in part at the Cornell NanoScale Facility, a member of the National Nanotechnology Infrastructure Network, which is supported by the National Science Foundation. This work made use of the TEM facility of the Cornell Center for Materials Research (CCMR) with support from the National Science Foundation Materials Research Science and Engineering Centers (MRSEC) program.